

Electronic Supplementary Information for:

**To Initiate Radical Photopolymerization with Long-Lived Triplet  
Charge-Separated State of Electron Donor–Acceptor Thermally  
Activated Delayed Fluorescence (TADF) Compounds**

Yuying Pei,<sup>[a,b]</sup> Xi Chen,<sup>[a]</sup> Yuqi Hou,<sup>[c]</sup> Jianzhang Zhao,<sup>\*[a]</sup> Yanqin Li,<sup>\*[b]</sup> and Shaomin Ji<sup>\*[d]</sup>

<sup>a</sup> State Key Laboratory of Fine Chemicals, Frontier Science Center for Smart Materials, School of Chemical Engineering, Dalian University of Technology, 2 Ling Gong Road, Dalian 116024 (P. R. China). E-mail: zhaojzh@dlut.edu.cn

<sup>b</sup> School of Chemistry, Dalian University of Technology, 2 Ling Gong Road, Dalian 116024 (P. R. China). E-mail: liyanqin@dlut.edu.cn

<sup>c</sup> School of Chemical Engineering, Ocean and Life Sciences, Dalian University of Technology, Panjin 124221 (P. R. China)

<sup>d</sup> School of Chemical Engineering and Light Industry, Guangdong University of Technology, Guangzhou 510006 (P. R. China). E-mail: smji@gdut.edu.cn

## Index

1. General Method and Synthesis.....	S3
2. Molecular Structure Characterization Data.....	S7
3. UV–Vis Absorption Spectra and Photobleaching.....	S13
4. Fluorescence and Fluorescence Lifetime Quenching.....	S15
5. Low-temperature Luminescence and Lifetime.....	S17
6. Cyclic Voltammograms and Spectroelectrochemistry.....	S18
7. Nanosecond Transient Absorption (ns-TA) Spectra.....	S20
8. Photopolymerization Kinetic Investigations.....	S23
9. References.....	S24

## 1. General Method and Synthesis

All the chemicals used in the synthesis were analytically pure and were used as received, without further purification. UV–vis absorption spectra were measured on a UV-2550 spectrophotometer (Shimadzu Ltd., Japan). Fluorescence emission spectra were recorded on a FS5 spectrofluorometer (Edinburgh Instrument Ltd, U.K.). Luminescence lifetimes of the compounds were obtained on OB920 luminescence lifetime spectrometer (Edinburgh Instruments Ltd., U.K.).

**1.1. Nanosecond Transient Absorption (ns TA) Spectroscopy.** The ns TA spectra were obtained on LP920 and LP980 laser flash photolysis spectrometers (Edinburgh Instruments, U.K.). Samples were purged with N<sub>2</sub> for 10 min before measurements, and then excited with a nanosecond pulsed laser (Quantel Nd:YAG nanosecond pulsed laser for LP980, Surelite OPO Plus SL I-10, Continuum Ltd., USA). The transient signals were digitized with a Tektronix TDS 3012B oscilloscope and the data were processed with L900 software.

**1.2. Electrochemical Studies.** Cyclic voltammograms curves were measured with a CHI610D electrochemical workstation (CHI instruments, Inc., Shanghai, China). Before starting the test, the samples were purged with N<sub>2</sub> for 10 min and nitrogen atmosphere was maintained during the measurement. 0.10 M Bu<sub>4</sub>N[PF<sub>6</sub>] was used as a supporting electrolyte, the counter electrode was a platinum electrode, glassy carbon electrode as the working electrode and the Ag/AgNO<sub>3</sub> (0.1 M in acetonitrile (ACN)) couple was used as the reference electrode. Ferrocenium/ferrocene (Fc<sup>+</sup>/Fc) redox couple was used as an internal reference.

**1.3. Photopolymerization Kinetic investigations.**<sup>1</sup> The photopolymerization kinetic curves were continuously followed by real time FT-IR spectroscopy (Thermo Scientific Nicolet iS20). The irradiation light source was a 365 nm LED with an irradiation intensity of 30 mW/cm<sup>2</sup>, and a homogeneous liquid including photosensitizer, co-initiator and monomers was spread evenly on the surface, which was covered with a slide to isolate oxygen.

The change of double band conversion (DC) with time was determined by monitoring the change of

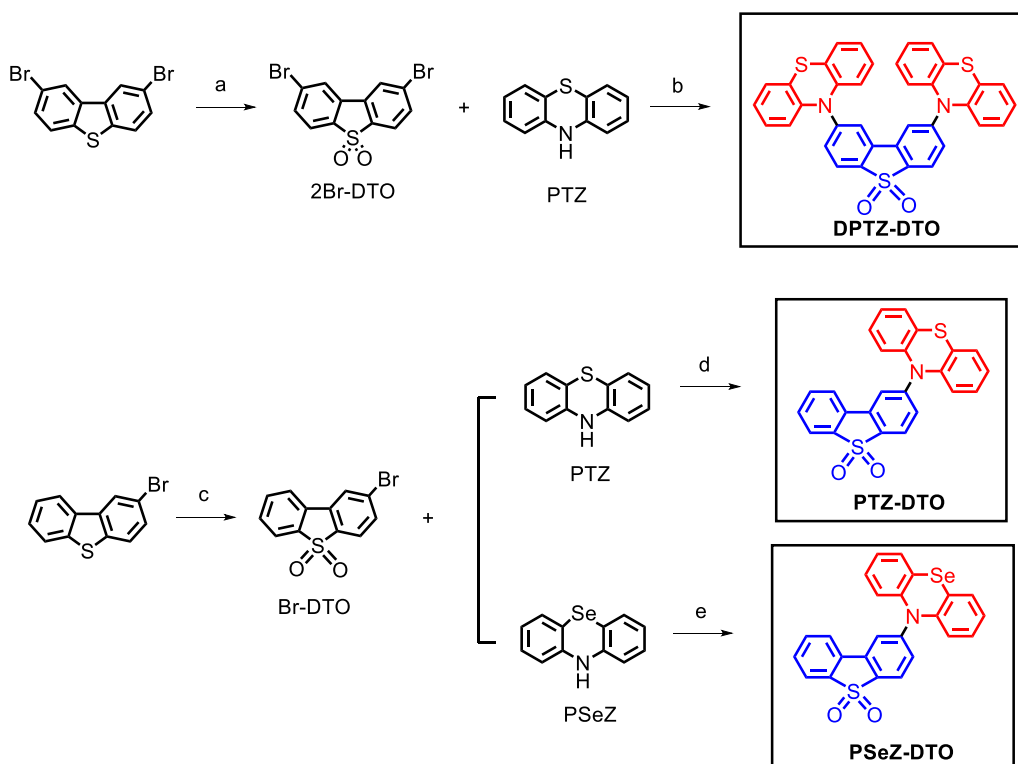
the C=C stretching vibrational absorption peak centered at 1630 cm<sup>-1</sup> and taking C=O centered at 1760 cm<sup>-1</sup> as internal standard. The calculation formula was shown below:

$$\text{Conversion (\%)} = \left(1 - \frac{A_t}{A_0}\right) \times 100\% \quad (1)$$

where  $A_0$  and  $A_t$  represents the ratio of the relative absorption band areas before photopolymerization and at photopolymerization time  $t$ , respectively.

**1.4 Photolithography.** The photosensitizer, polyacrylic acid and photoinitiator were dissolved in a small amount of solvent and then mixed thoroughly with PETA monomer. Then drop the mixed solution into the center of the wafer with a pipette gun for spin coating. Then, it was pre-baked at 100 °C for 2 min. Subsequently, it was exposed at 365 nm UV light for 100 s. Finally, the wafer was developed with isopropanol, and the obtained patterns were photographed. Photolithographic patterns were acquired by scanning electron microscope (QUANTA 450, FEI, USA) and metallographic microscope (Axio Scope 5, Carl Zeiss AG, GER).

### 1.5 Synthesis Details.



**Scheme S1:** <sup>a</sup>Key: (a) HAc, H<sub>2</sub>O<sub>2</sub>, refluxed, 30 min, yield: 94%; (b) Pd<sub>2</sub>(dba)<sub>3</sub>, XPhos, *t*-BuONa, toluene (TOL), 110 °C, 8 h, under N<sub>2</sub>, yield: 46%; (c) similar to step (a), yield: 98%; (d) similar to step (b), yield: 85%; (e) Pd(OAc)<sub>2</sub>, *t*-BuONa, Tri-*tert*-butylphosphine tetrafluoroborate, TOL, 110 °C, 8 h, under N<sub>2</sub>, yield: 30%. PSeZ were synthesized according to literature method.<sup>2,3</sup>

**Synthesis of PTZ-DTO.**<sup>4</sup> **Br-DTO** (1.2 g, 4.00 mmol), PTZ (836.0 mg, 4.20 mmol) were dissolved in dry TOL (100 mL). Then Pd<sub>2</sub>(dba)<sub>3</sub> (74.0 mg, 0.08 mmol), XPhos (192.0 mg, 0.4 mmol) and *t*-BuONa (576.0 mg, 6.00 mmol) were added under N<sub>2</sub> atmosphere. The mixture was refluxed and stirred for 8 h. After the reaction finished, cooling to room temperature, water (5 mL) was added and the mixture was extracted with dichloromethane (3 × 20 mL). The organic layer was dried over anhydrous Na<sub>2</sub>SO<sub>4</sub> and the solvent was evaporated under reduced pressure. The crude product was purified by column chromatography (silica gel, dichloromethane: petroleum ether = 2: 1, v: v). Compound **PTZ-DTO** was obtained as white solid. Yield: 1.4 g (85%). <sup>1</sup>H NMR (400 MHz, DMSO) δ 8.10–8.05 (m, 2H), 7.99 (d, *J* = 6.3 Hz, 2H), 7.79–7.75 (m, 1H), 7.69–7.65 (m, 1H), 7.42–7.37 (m, 3H), 7.25–7.21 (m, 2H), 7.15–7.11 (m, 2H), 6.93 (d, *J* = 8.0 Hz, 2H). ESI HRMS(C<sub>24</sub>H<sub>15</sub>NO<sub>2</sub>S<sub>2</sub>+Na<sup>+</sup>) *m/z*. calcd: 436.0436; found: 436.0444.

**Synthesis of PSeZ-DTO.**<sup>5</sup> **Br-DTO** (236.0 mg, 0.80 mmol), PSeZ (216.6 mg, 0.88 mmol), Pd(OAc)<sub>2</sub> (9.0 mg, 0.04 mmol) and *t*-BuONa (115.3 mg, 1.20 mmol) were mixed in dry TOL (15 mL). Then tri-*tert*-butylphosphine tetrafluoroborate (58.0 mg, 0.20 mmol) was added under N<sub>2</sub> atmosphere. The reaction mixture was heated to 120 °C and stirred for 8 h. After cooling, the product was extracted with dichloromethane and water, and dried with anhydrous sodium sulfate. The solvent was then evaporated under reduced pressure. The crude product was purified by column chromatography (silica gel, EA: petroleum ether = 1:10, v: v). Compound **PSeZ-DTO** was obtained as white solid. Yield: 50.0 mg (30%). <sup>1</sup>H NMR (400 MHz, DMSO) δ 7.91 (d, *J* = 7.6 Hz, 1H), 7.81–7.76 (m, 4H), 7.72–7.69 (m, 1H), 7.65–7.61 (m, 3H), 7.52–7.50 (m, 2H), 7.37–7.33 (m, 3H), 6.94 (d, *J* = 8.5 Hz, 1H). <sup>13</sup>C NMR (126 MHz, CDCl<sub>3</sub>): δ 151.17, 140.87, 138.93, 133.39, 133.29, 132.45, 131.90, 131.57, 130.24, 128.45, 128.20, 128.04, 127.14, 123.24, 121.87, 121.29, 114.99, 105.71. ESI HRMS(C<sub>24</sub>H<sub>15</sub>NO<sub>2</sub>S<sub>2</sub>Se+Na<sup>+</sup>) *m/z*. calcd: 483.9881; found: 483.9882.

**Synthesis of DPTZ-DTO.**<sup>6</sup> **2Br-DTO** (374.1 mg, 1.00 mmol), PTZ (419.0 mg, 2.10 mmol) were

mixed in dry TOL (10 mL). Then Pd<sub>2</sub>(dba)<sub>3</sub> (59.5 mg, 0.07 mmol), XPhos (62 mg, 0.13 mmol) and *t*-BuONa (211.4 mg, 2.20 mmol) were added under N<sub>2</sub> atmosphere. The mixture was refluxed and stirred for 8 h. After cooling to room temperature, water (5 mL) was added and the mixture was extracted with dichloromethane (3 × 20 mL). The organic layer was separated and washed with water and brine. The crude product was purified by column chromatography (silica gel, dichloromethane: petroleum ether = 2: 1, v: v). Compound **DPTZ-DTO** was obtained as white solid. Yield: 283.7 mg (46%). <sup>1</sup>H NMR (400 MHz, DMSO), δ 7.98 (d, *J* = 8.4 Hz, 2H), 7.69 (s, 2H), 7.39 (d, *J* = 7.5 Hz, 4H), 7.33 (d, *J* = 8.4 Hz, 2H), 7.27–7.23 (m, 4H), 7.18–7.15 (m, 4H), 7.01 (d, *J* = 7.9 Hz, 4H). ESI HRMS(C<sub>36</sub>H<sub>22</sub>N<sub>2</sub>O<sub>2</sub>S<sub>3</sub>+Na<sup>+</sup>) *m/z*. calcd: 633.0735; found: 633.0731.

**Synthesis of Br-DTO.**<sup>7</sup> Dibenzothiophene (5.26 g, 0.02 mmol) was dissolved in 20 ml HAc and 6 ml 30% H<sub>2</sub>O<sub>2</sub> was added at 80 °C. The solution was heated at 90 °C for 1 h and then refluxed for 30 min, 2 ml H<sub>2</sub>O<sub>2</sub> was added and refluxing was continued for 30 min. The mixture was cooled to room temperature and filtered. Compound **Br-DTO** was obtained as white solid. Yield: 4.5 g (98%). <sup>1</sup>H NMR (400 MHz, DMSO), δ 8.56 (s, 1H), 8.29 (d, *J* = 7.75 Hz, 1H), 8.02 (d, *J* = 7.63 Hz, 1H), 7.96 (d, *J* = 8.13 Hz, 1H), 7.87–7.82 (m, 2H), 7.72–7.68 (t, *J* = 7.56 Hz, 1H). HRMS (ESI): calcd for C<sub>12</sub>H<sub>7</sub>BrO<sub>2</sub>S<sup>+</sup>, *m/z* 293.9344; found [C<sub>12</sub>H<sub>7</sub>BrO<sub>2</sub>S+Na]<sup>+</sup>, *m/z* 316.9248.

**Synthesis of 2Br-DTO.**<sup>7</sup> The synthesis procedure is similar to that of **Br-DTO**. The product was obtained as white solid. Yield: 1.19 g (94%). <sup>1</sup>H NMR (400 MHz, DMSO), δ 8.64 (s, 2H), 7.99 (d, *J* = 8.25 Hz, 2H), 7.90 (d, *J* = 7.63 Hz, *J* = 8.26 Hz, 2H). HRMS (ESI): calcd for C<sub>12</sub>H<sub>6</sub>Br<sub>2</sub>O<sub>2</sub>S<sup>+</sup>, *m/z* 371.8449; found [C<sub>12</sub>H<sub>6</sub>Br<sub>2</sub>O<sub>2</sub>S+Na]<sup>+</sup>, *m/z* 394.8336.

## 2. Molecular Structure Characterization Data

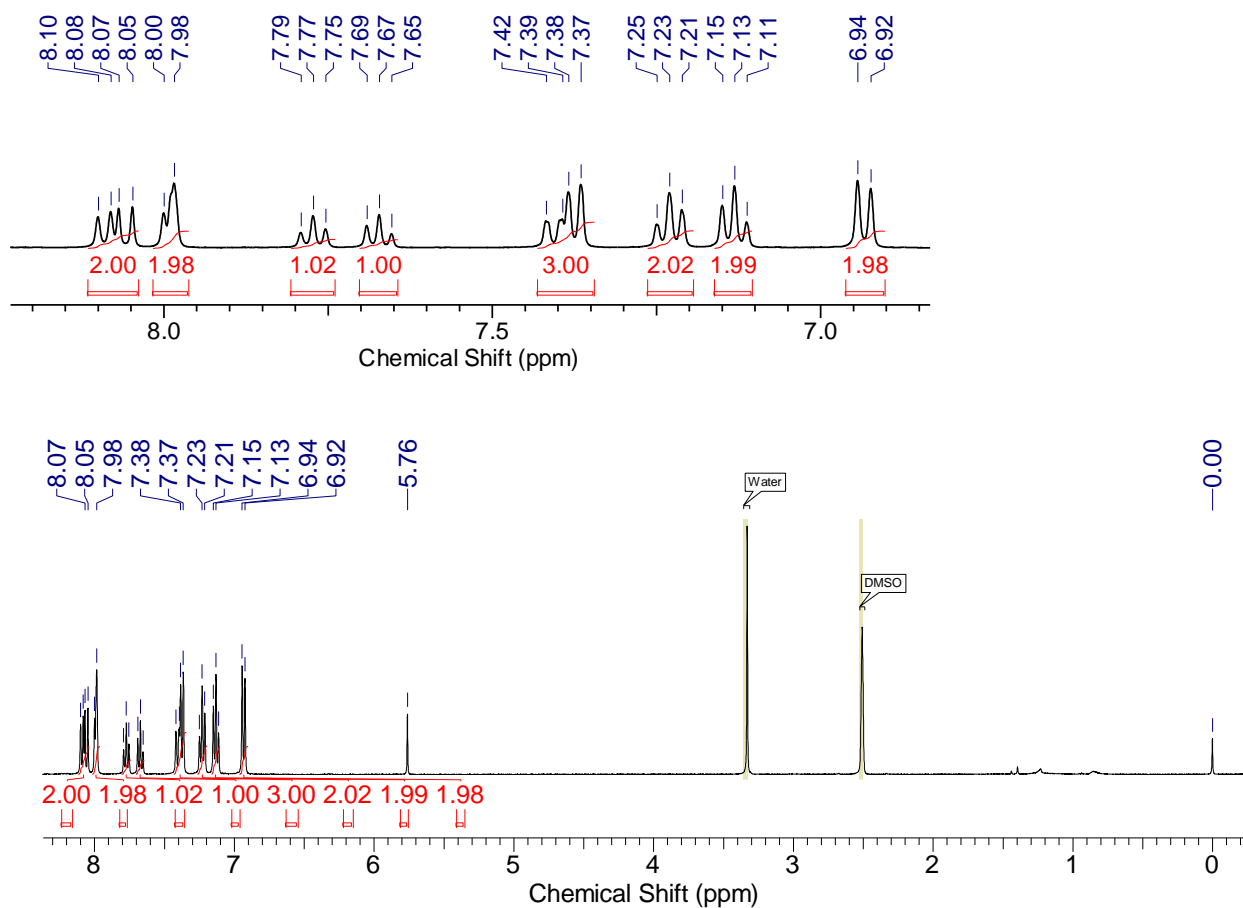


**Figure S1.**  $^1\text{H}$  NMR spectrum of compound **PTZ-DTO** (400 MHz,  $\text{DMSO}-d_6$ ).

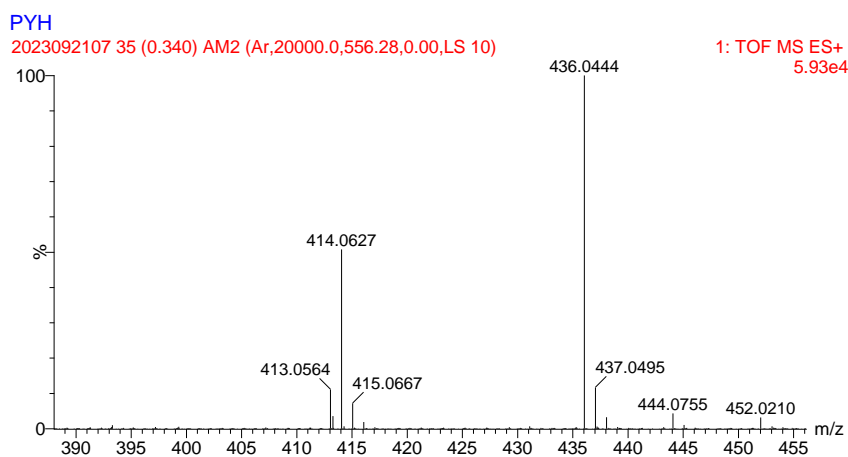


**Figure S2.** ESI-HRMS spectrum of compound **PTZ-DTO**.

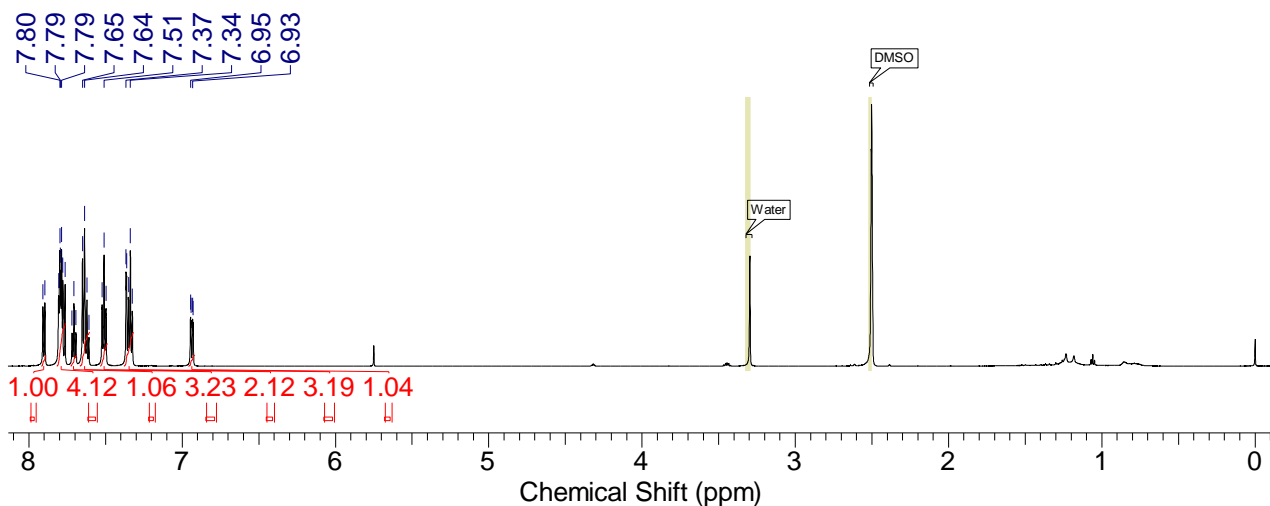
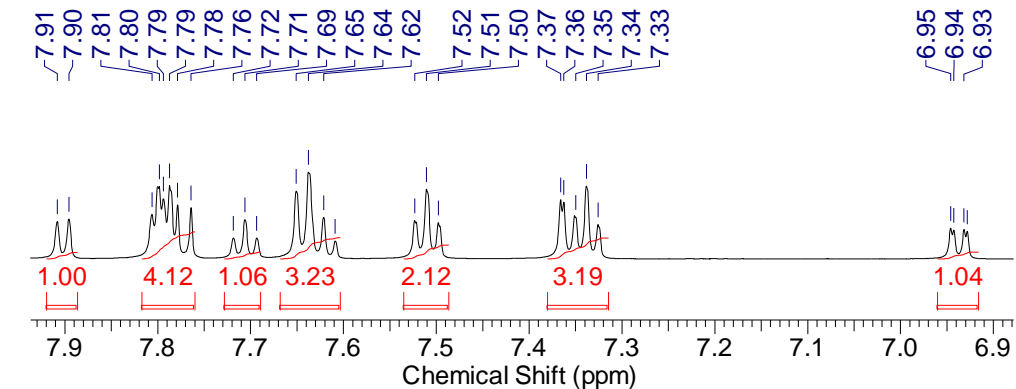


**Figure S3.**  $^1\text{H}$  NMR spectrum of compound **PSeZ-DTO** (400 MHz,  $\text{DMSO-}d_6$ ).

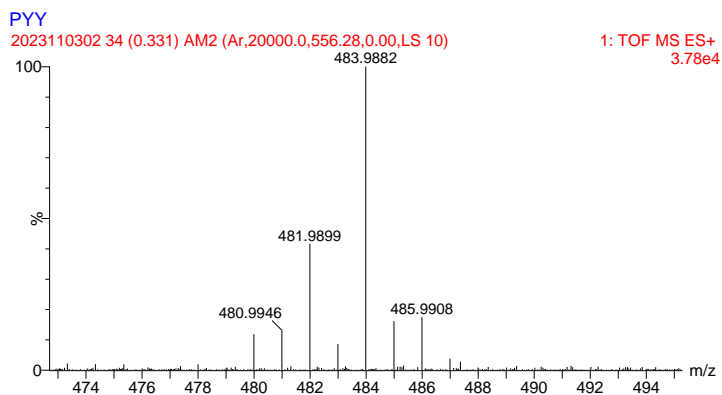


**Figure S4.** ESI-HRMS spectrum of compound **PSeZ-DTO**.

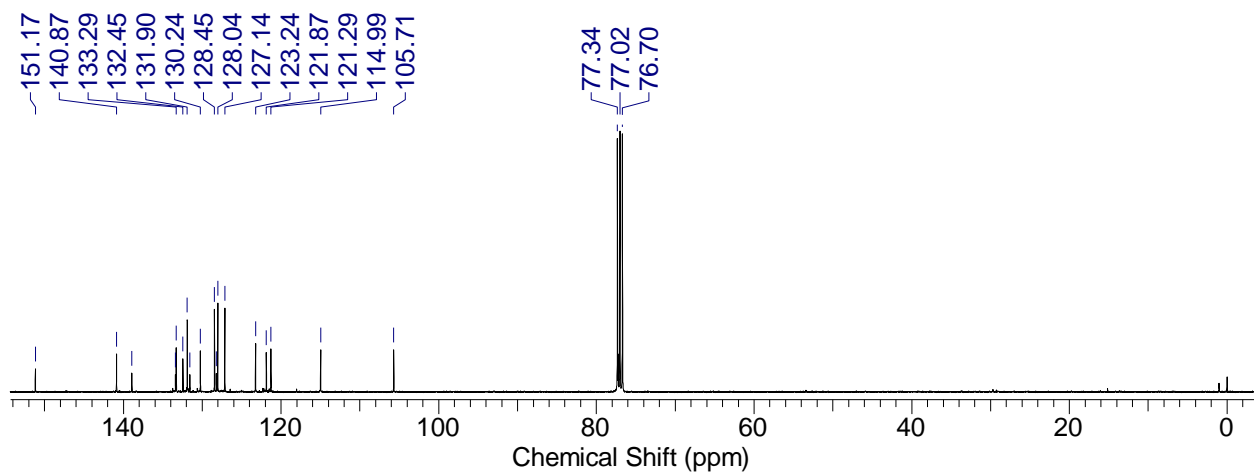
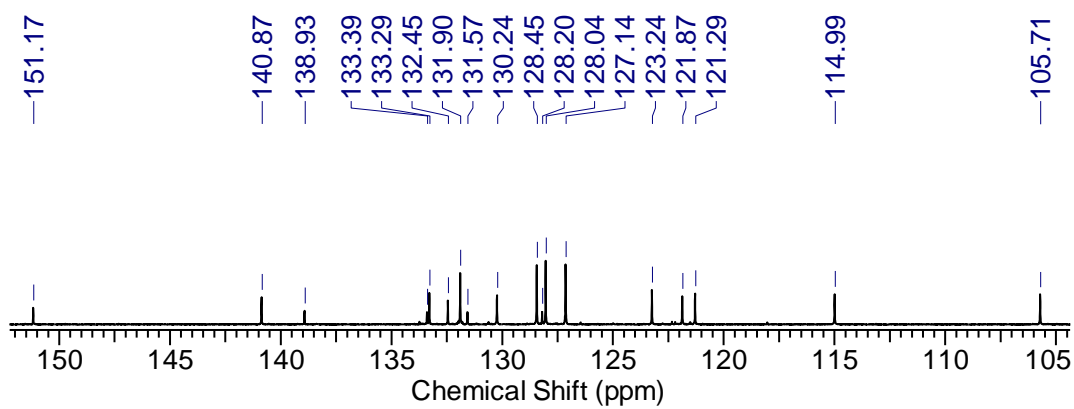


**Figure S5.** <sup>13</sup>C NMR spectrum of compound **PSeZ-DTO** (100 MHz, CDCl<sub>3</sub>).

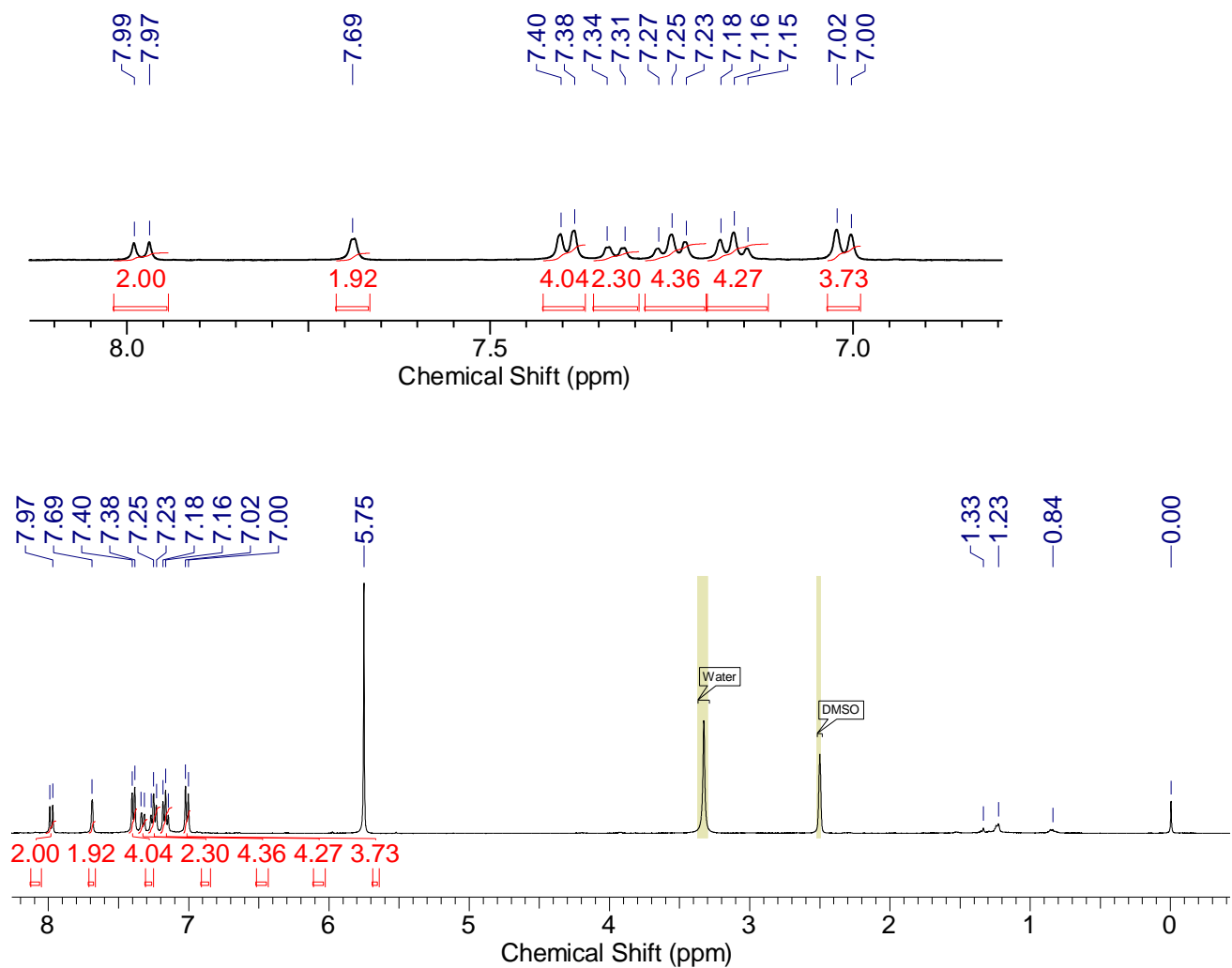


**Figure S6.**  $^1\text{H}$  NMR spectrum of compound **DPTZ-DTO** (400 MHz,  $\text{DMSO-}d_6$ ).

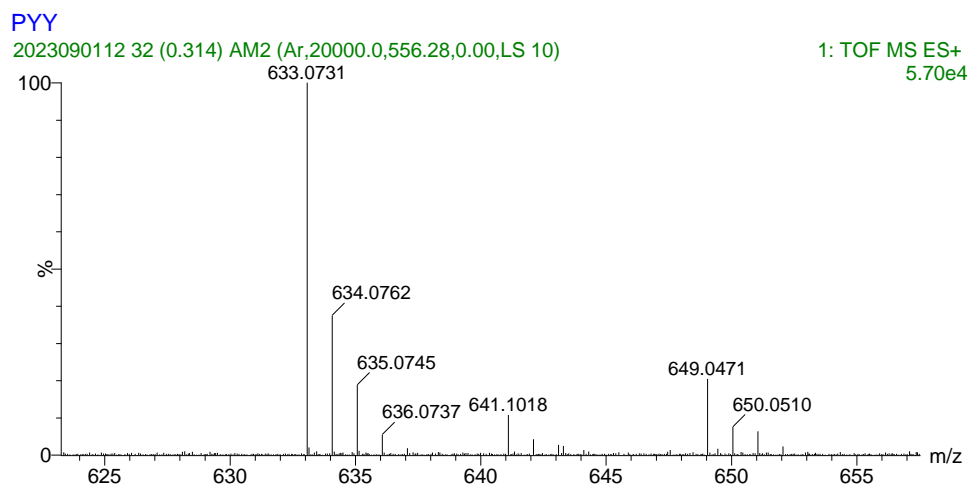


**Figure S7.** ESI-HRMS spectrum of compound **DPTZ-DTO**.

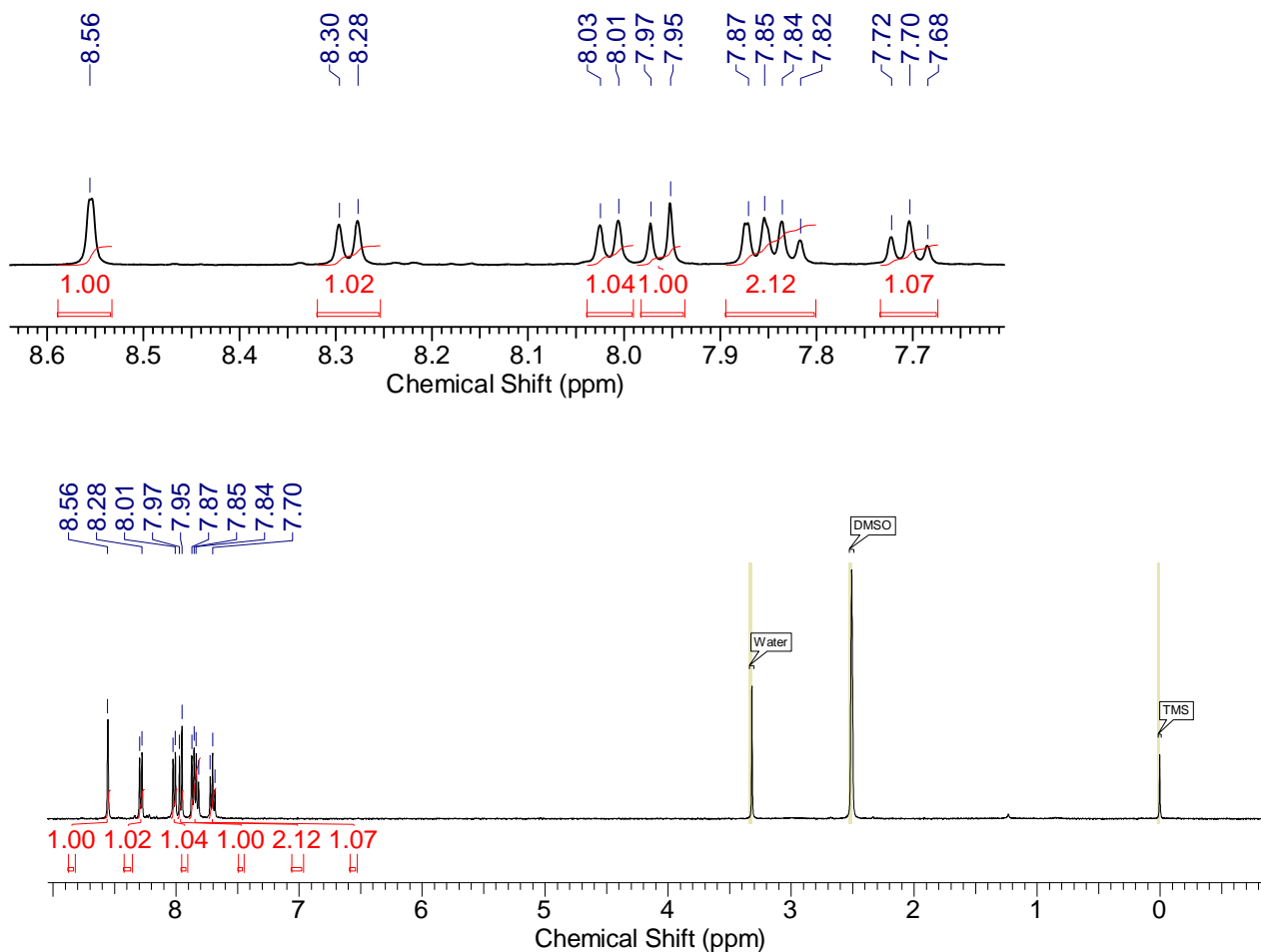


**Figure S8.** <sup>1</sup>H NMR spectrum of compound **Br-DTO** (400 MHz, DMSO-*d*<sub>6</sub>).

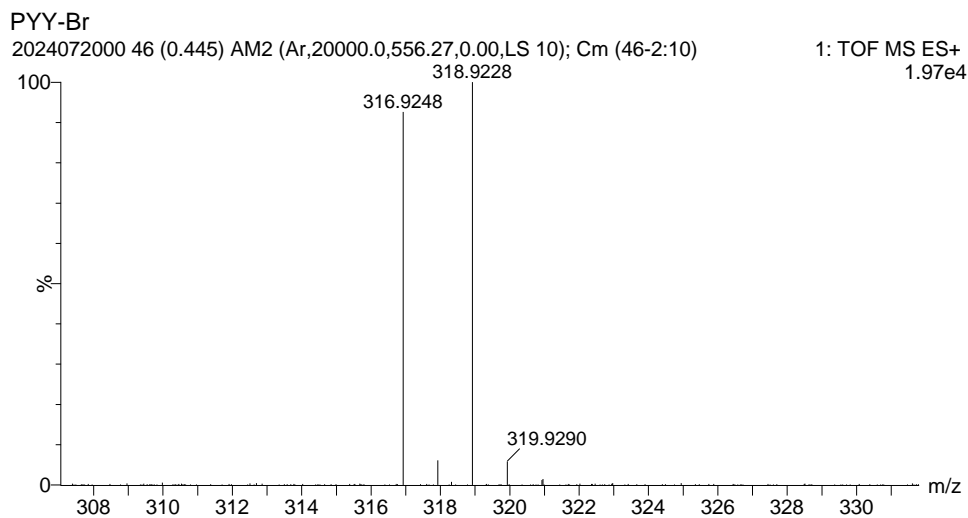


**Figure S9.** ESI-HRMS spectrum of compound **Br-DTO**.

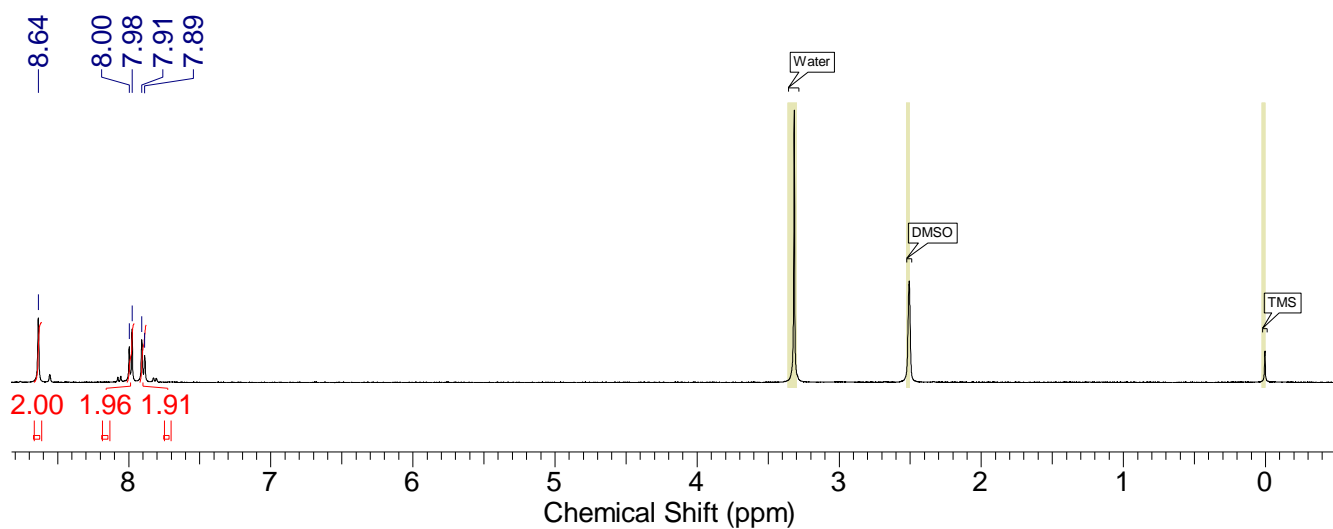
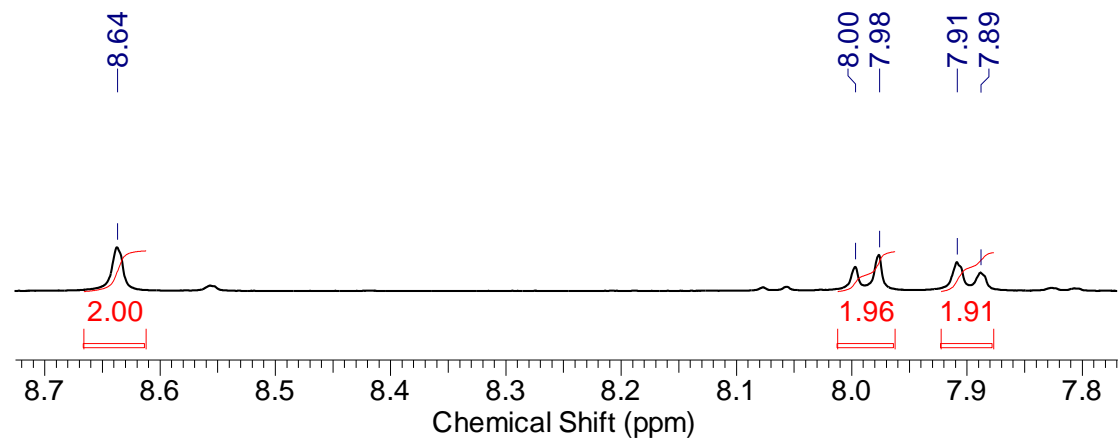


**Figure S10.**  $^1\text{H}$  NMR spectrum of compound **2Br-DTO** (400 MHz,  $\text{DMSO}-d_6$ ).

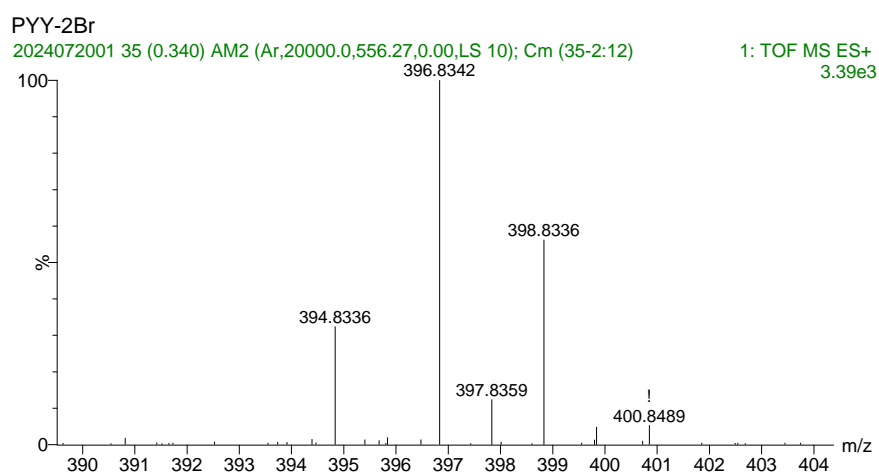


**Figure S11.** ESI-HRMS spectrum of compound **2Br-DTO**.

### 3. UV–Vis Absorption Spectra and Photobleaching

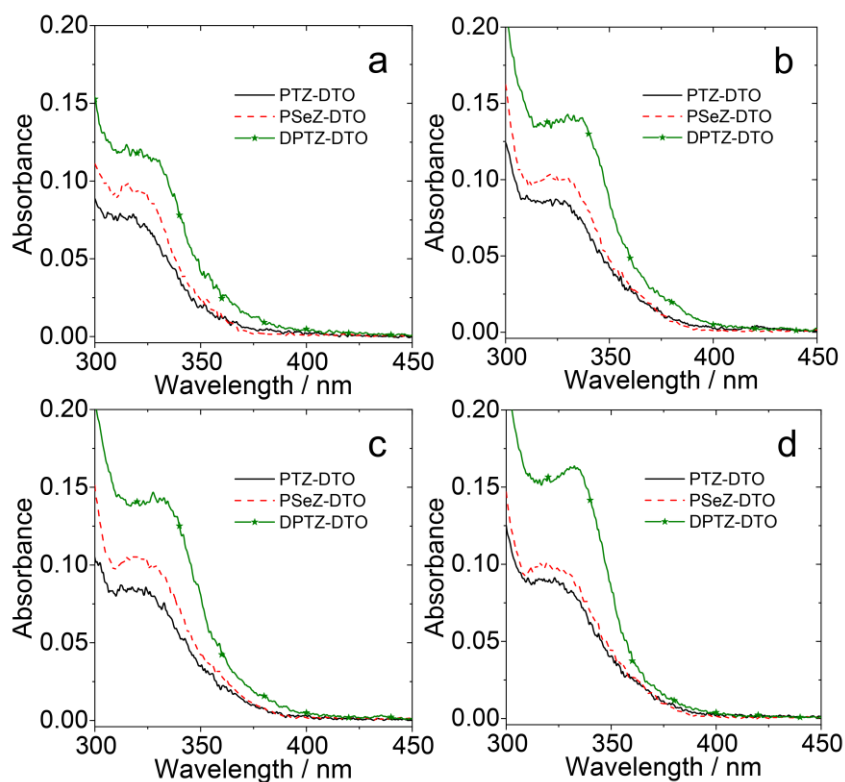


**Figure S12.** UV–vis absorption spectra of **PTZ-DTO**, **PSeZ-DTO** and **DPTZ-DTO** in (a) hexane (HEX), (b) dichloromethane (DCM), (c) acetonitrile (ACN) and (d) methanol (MeOH).  $c = 1.0 \times 10^{-5}$  M, 25 °C.

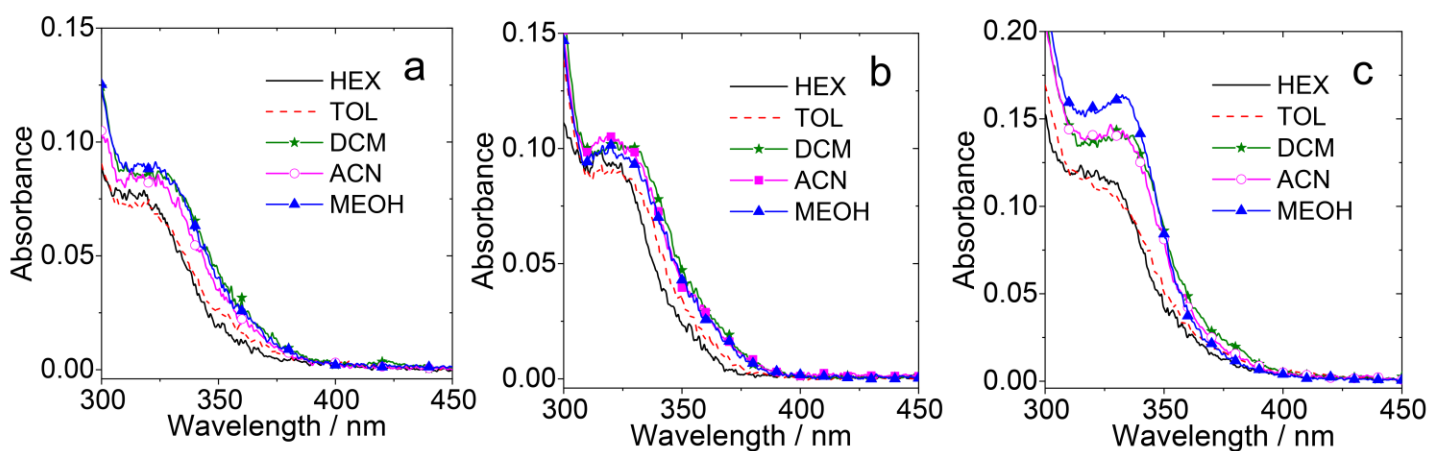


**Figure S13.** UV–vis absorption spectra of (a) **PTZ-DTO**, (b) **PSeZ-DTO** and (c) **DPTZ-DTO** in different solvents.  $c = 1.0 \times 10^{-5}$  M, 25 °C.

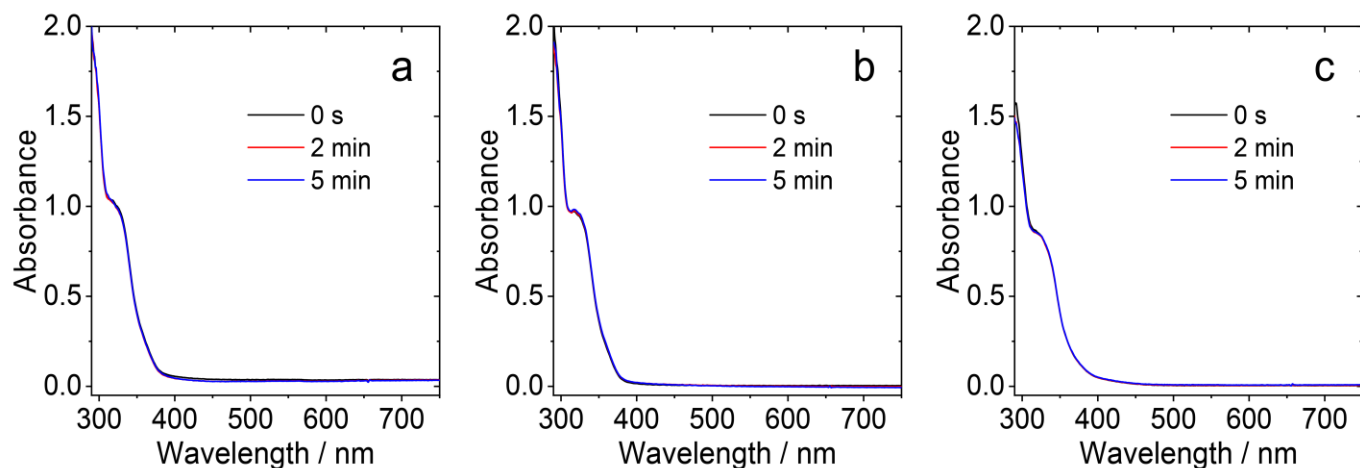


**Figure S14.** UV-vis absorption spectra of (a) **PTZ-DTO** ( $1.4 \times 10^{-4}$  M), (b) **PSeZ-DTO** ( $1.1 \times 10^{-4}$  M) and (c) **DPTZ-DTO** ( $7.6 \times 10^{-5}$  M) upon 365 nm LED exposure in deaerated TOL, the power density is  $50 \text{ mW/cm}^{-2}$ ,  $25^\circ\text{C}$ .

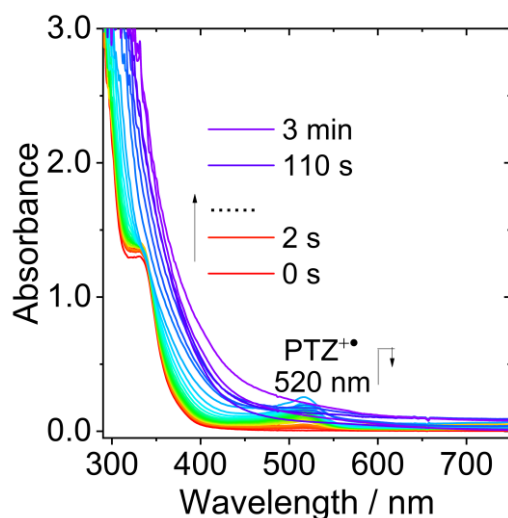


**Figure S15.** UV-vis absorption spectra of **DPTZ-DTO** ( $1.9 \times 10^{-4}$  M) upon 365 nm LED exposure in the presence of DPI in deaerated TOL,  $c[\text{DPI}] = 1.0 \times 10^{-3}$  M, the power density is  $50 \text{ mW/cm}^{-2}$ ,  $25^\circ\text{C}$ .

#### 4. Fluorescence and Fluorescence Lifetime quenching

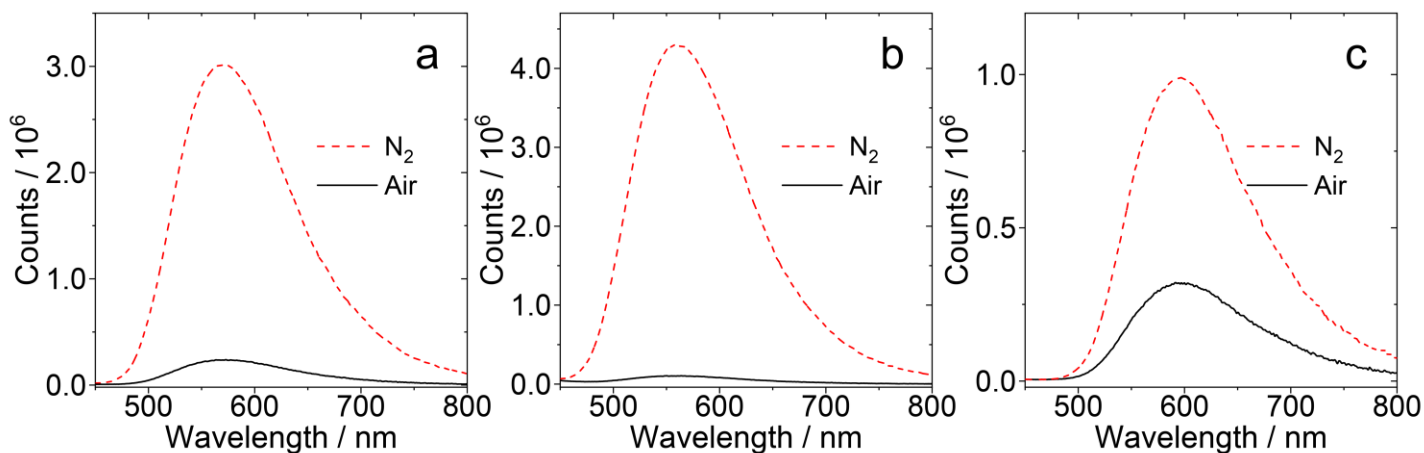


**Figure S16.** Fluorescence spectra of (a) **PTZ-DTO**, (b) **PSeZ-DTO** and (c) **DPTZ-DTO** under N<sub>2</sub> and air atmospheres in TOL.  $\lambda_{\text{ex}} = 310 \text{ nm}$ ,  $A = 0.10$ ,  $c \approx 1.0 \times 10^{-5} \text{ M}$ .

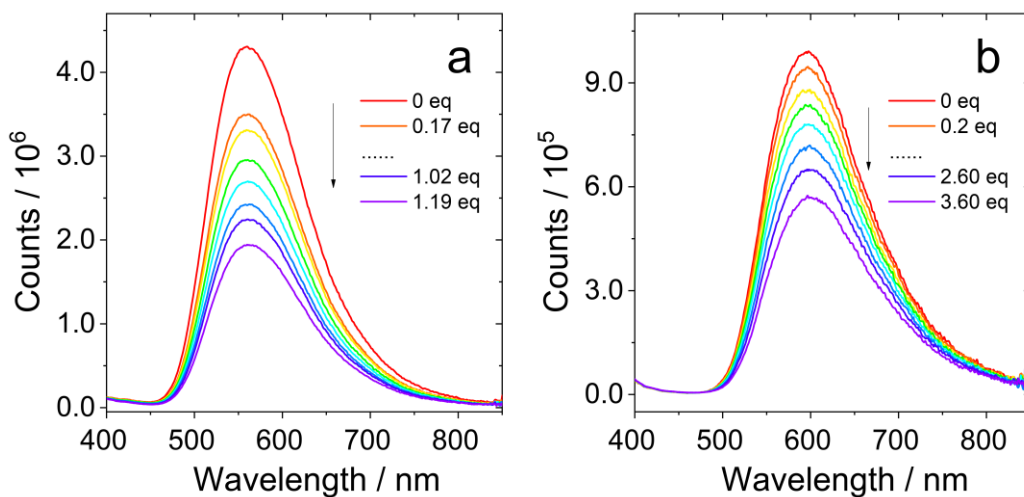


**Figure S17.** Fluorescence quenching spectra of (a) **PSeZ-DTO** and (b) **DPTZ-DTO** under N<sub>2</sub> atmospheres in TOL upon the increasing addition of DPI.  $\lambda_{\text{ex}} = 310 \text{ nm}$ ,  $A = 0.10$ ,  $c \approx 1.0 \times 10^{-5} \text{ M}$ .

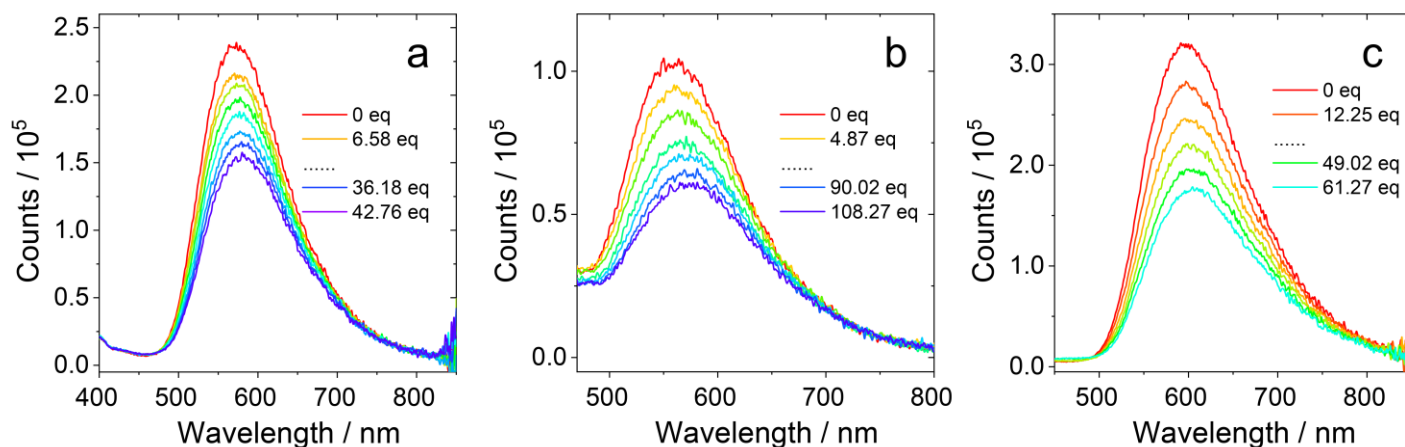


**Figure S18.** Fluorescence quenching spectra of (a) **PTZ-DTO**, (b) **PSeZ-DTO** and (c) **DPTZ-DTO** under Air atmospheres in TOL upon the increasing addition of DPI.  $\lambda_{ex} = 310$  nm,  $A = 0.10$ ,  $c \approx 1.0 \times 10^{-5}$  M.

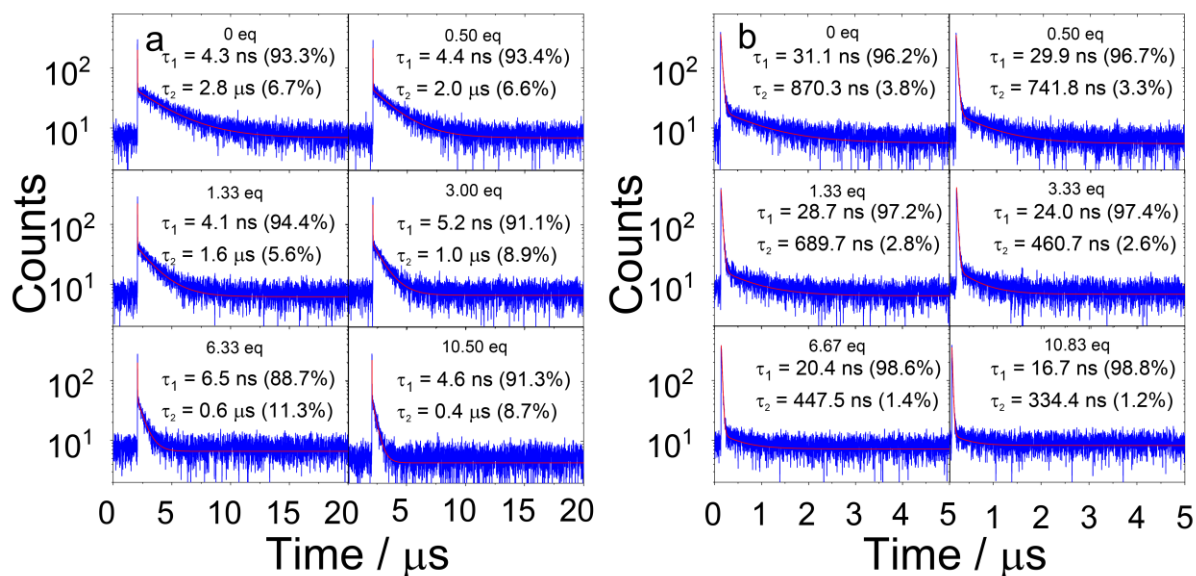


**Figure S19.** Fluorescence decay traces of (a) **PSeZ-DTO** at 550 nm and (b) **DPTZ-DTO** at 580 nm under N<sub>2</sub> atmospheres in TOL upon the increasing addition of DPI,  $c = 1.0 \times 10^{-5}$  M,  $\lambda_{ex} = 340$  nm.

## 5. Low-temperature Luminescence and Lifetime

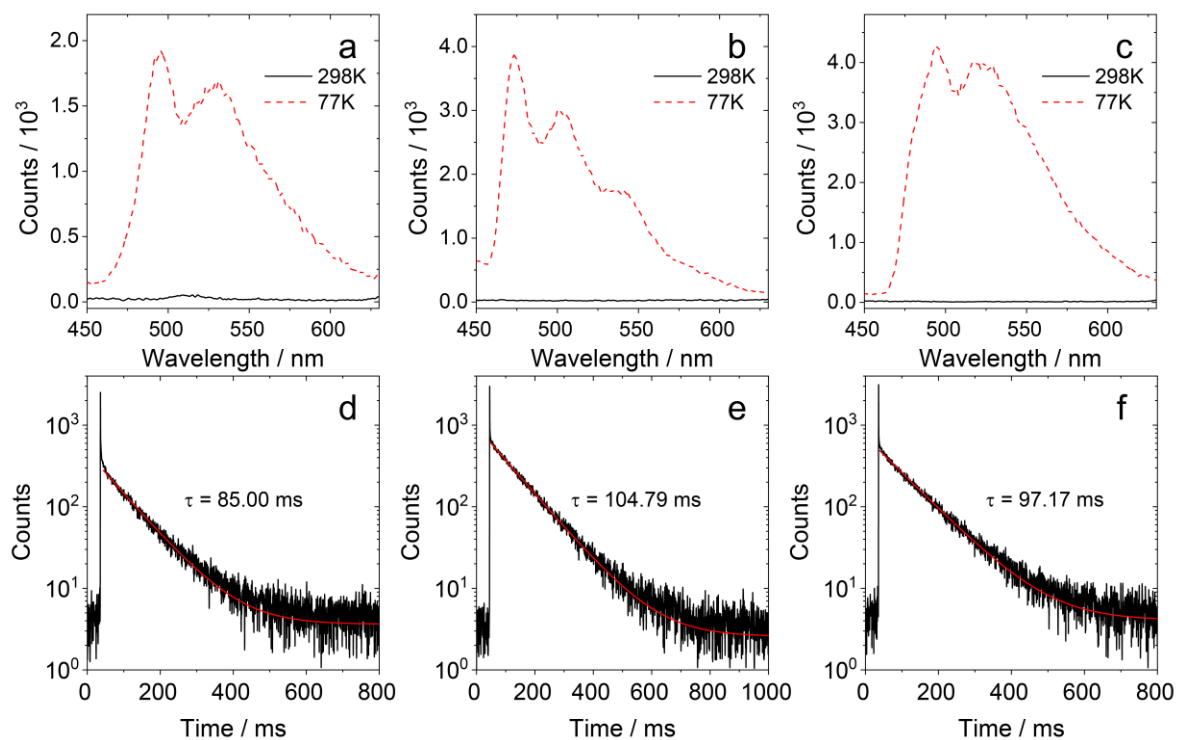


**Figure S20.** (a) Luminescence of (a) **PTZ-DTO**, (b) **PSeZ-DTO** and (c) **DPTZ-DTO** at room temperature and low-temperature. Lifetime of (d) **PTZ-DTO** monitor at 495 nm, (e) **PSeZ-DTO** monitor at 475 nm and (f) **DPTZ-DTO** monitor at 495 nm at 77K in deaerated MeTHF.  $c = 1.0 \times 10^{-4}$  M,  $\lambda_{ex} = 340$  nm, 25 °C.

## 6. Cyclic Voltammograms and Spectroelectrochemistry

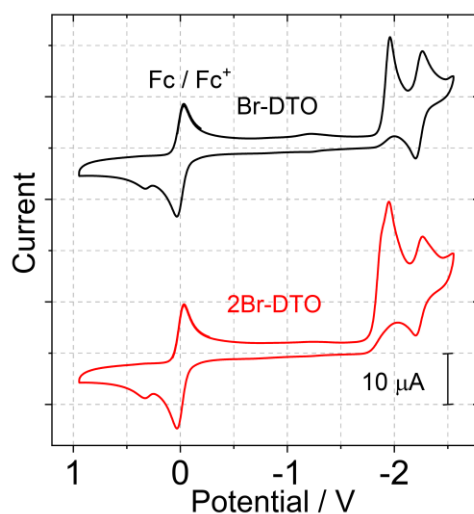


**Figure S21.** Cyclic voltammograms of **Br-DTO** and **2Br-DTO** in deaerated ACN solutions,  $c = 1.0 \times 10^{-3}$  M. 0.10 M  $\text{Bu}_4\text{NPF}_6$  was used as the supporting electrolyte and  $\text{Ag}/\text{AgNO}_3$  was used as the reference electrode. Scan rates: 50 mV/s. Ferrocene (Fc) was used as an internal reference.

**Table S1.** Redox Potentials of the Compounds.<sup>[a]</sup>

	<b>Br-DTO</b>	<b>2Br-DTO</b>
$E_{\text{ox}}(\text{V})$	— <sup>[b]</sup>	— <sup>[b]</sup>
$E_{\text{red}}(\text{V})$	-1.96	-1.96
	-2.24	-2.24

[a] Cyclic voltammetry in deaerated solutions containing a 0.10 M  $\text{Bu}_4\text{NPF}_6$ . Pt electrode is counter electrode, glassy carbon electrode is working electrode, and  $\text{Ag}/\text{AgNO}_3$  couple as the reference electrode; [b] Not observed.

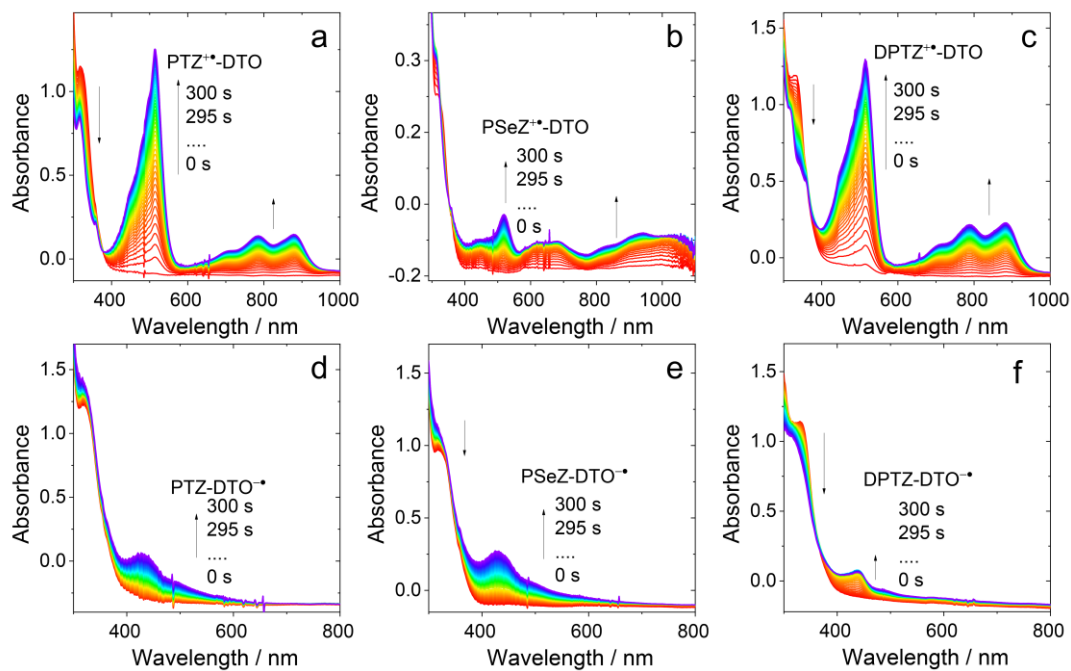


**Figure S22.** The UV-vis absorption changes of **PTZ-DTO** upon (a) oxidation under 0.85 V ( $c = 1.6 \times 10^{-3}$  M), (d) reduction under  $-2.07$  V ( $c = 1.7 \times 10^{-3}$  M). **PSeZ-DTO** upon (b) oxidation under 0.50 V ( $c = 2.4 \times 10^{-4}$  M), (e) reduction under  $-2.12$  V ( $c = 1.1 \times 10^{-3}$  M). **DPTZ-DTO** upon (c) oxidation under 0.58 V ( $c = 1.1 \times 10^{-3}$  M), (f) reduction under  $-2.07$  V ( $c = 1.1 \times 10^{-3}$  M). The potentials are versus Ag/AgNO<sub>3</sub>. The spectra were recorded in situ with a spectroelectrochemical cuvette (1 mm optical path) in deaerated ACN. 25 °C.

## 7. Nanosecond Transient Absorption (ns-TA) Spectra

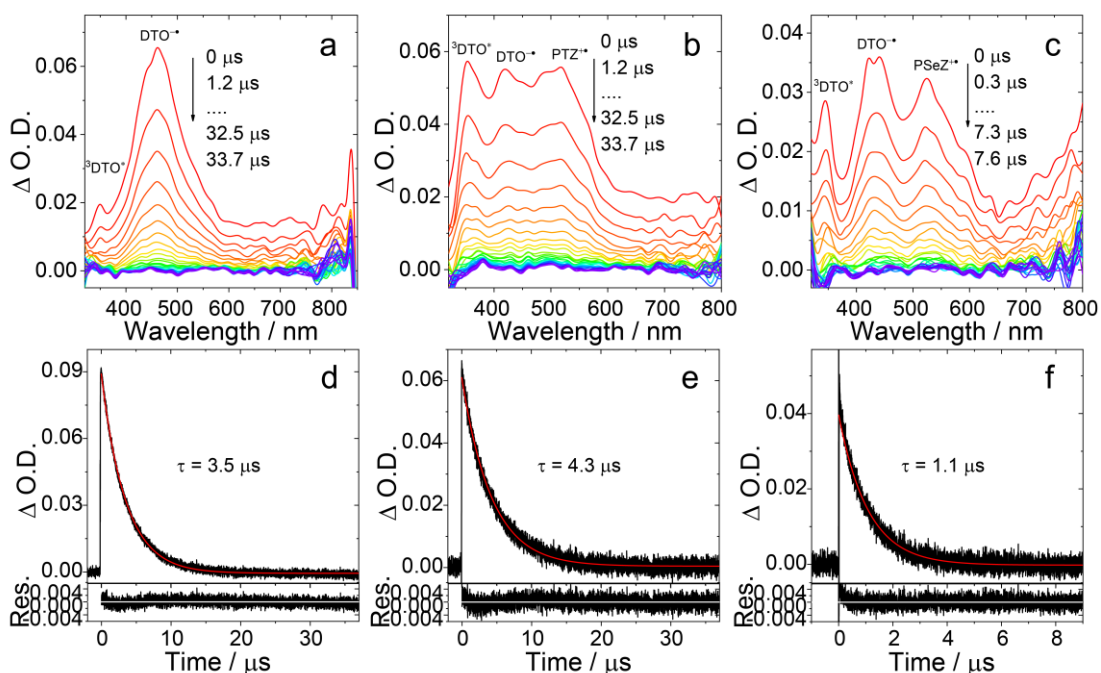


**Figure S23.** Nanosecond transient absorption spectra of the dyads. Transient absorption spectra of (a) **PTZ-DTO**, (b) **PSeZ-DTO**, (c) **DPTZ-DTO** and decay curves of (d) **PTZ-DTO** at 460 nm, (e) **PSeZ-DTO** at 420 nm, (c) **DPTZ-DTO** at 430 nm after pulsed laser excitation at 355 nm,  $c = 2.0 \times 10^{-5}$  M.

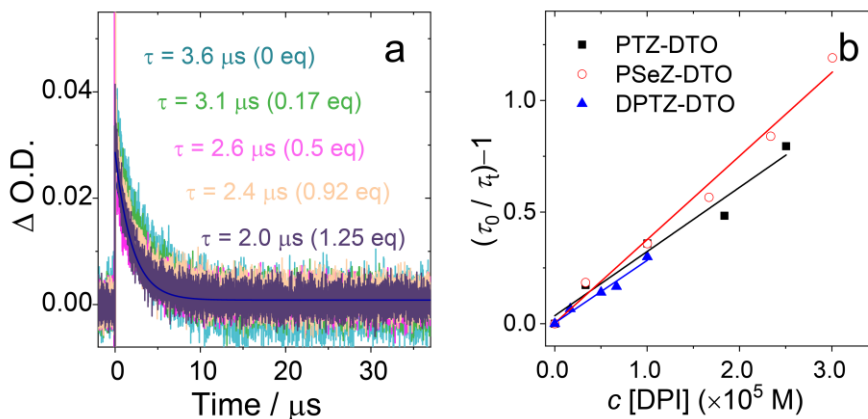


**Figure S24.** The decay traces of (a) **PTZ-DTO** ( $2.0 \times 10^{-5}$  M) at 350 nm in TOL upon incremental addition of DPI and (b) the corresponding Stern–Volmer plot for quenching of the **PTZ-DTO**, **PSeZ-DTO** and **DPTZ-DTO** of  $^3LE$  state,  $\lambda_{ex} = 355$  nm. All solvents used in measurements are deaerated, 25 °C.

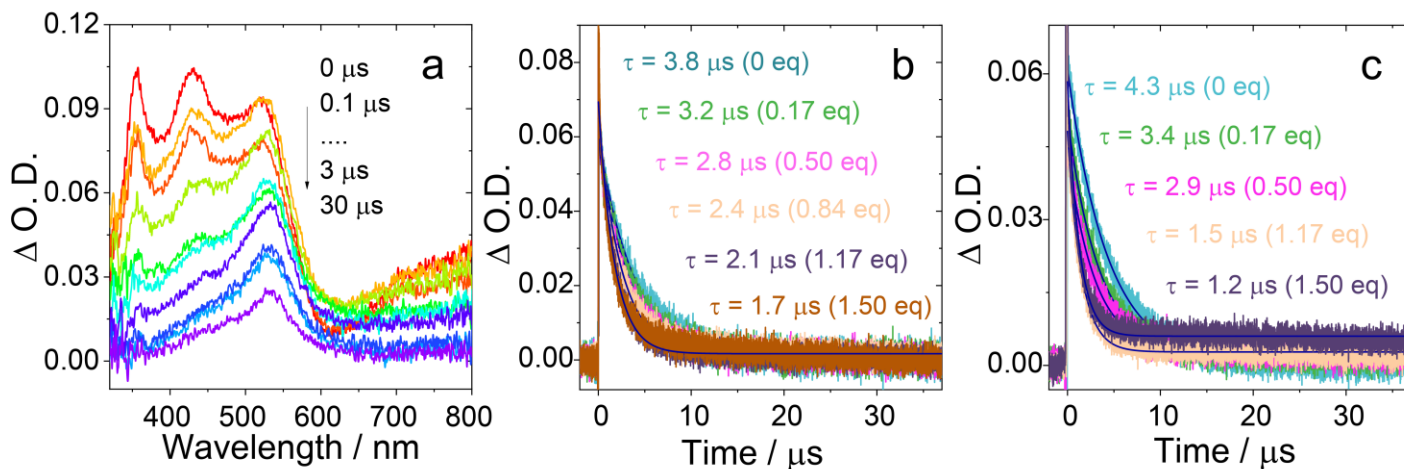


**Figure S25.** (a) Nanosecond transient absorption spectra of **PSeZ-DTO** ( $6.0 \times 10^{-5}$  M) at different delay times after laser flash in TOL,  $c$  (DPI) =  $1.3 \times 10^{-4}$  M. The decay traces of **PSeZ-DTO** ( $2.0 \times 10^{-5}$  M) at (b) 350 nm and (c) 420 nm in TOL upon incremental addition of DPI.

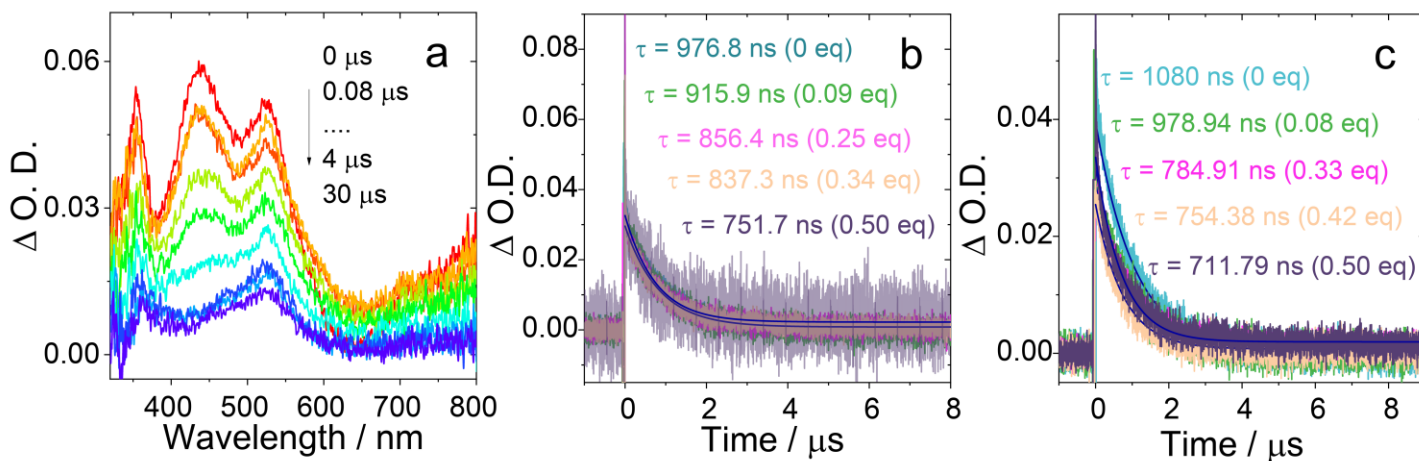


**Figure S26.** (a) Nanosecond transient absorption spectra of **DPTZ-DTO** ( $6.0 \times 10^{-5}$  M) at different delay times after laser flash in TOL,  $c$  (DPI) =  $5.4 \times 10^{-5}$  M. The decay traces of **DPTZ-DTO** ( $2.0 \times 10^{-5}$  M) at (b) 350 nm and (c) 430 nm in TOL upon incremental addition of DPI.

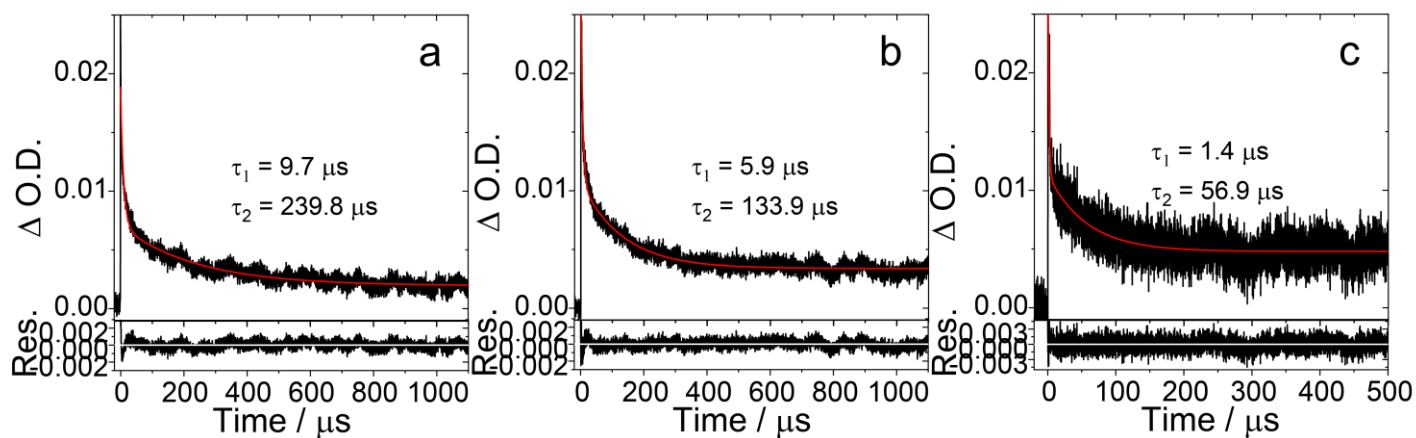


**Figure S27.** The decay traces of (a) **PTZ-DTO**, (b) **PSeZ-DTO** and (c) **DPTZ-DTO** ( $2.0 \times 10^{-5}$  M) at 520 nm in TOL upon addition of DPI ( $5 \times 10^{-5}$  M).

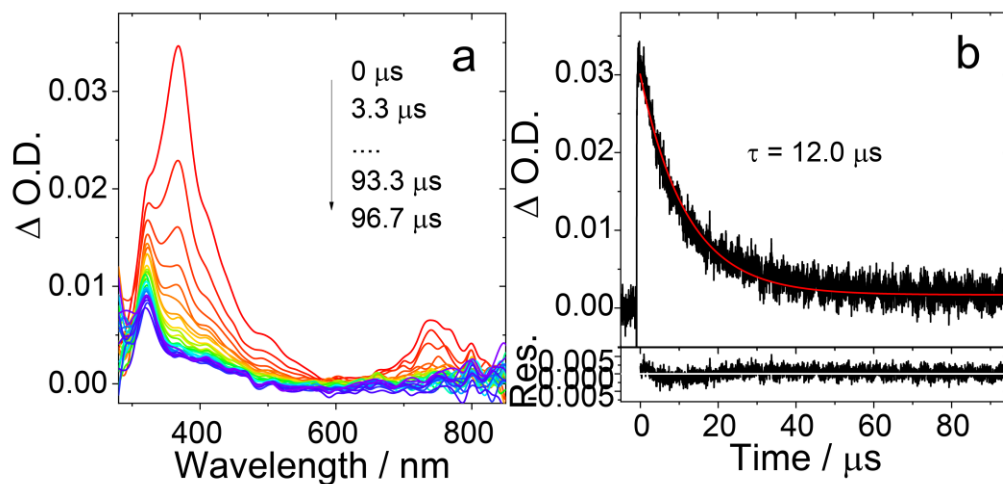


**Figure S28.** Nanosecond transient absorption spectra of the dyads. Transient absorption spectra of **Br-DTO** and decay curves of **Br-DTO** at 350 nm after pulsed laser excitation at 266 nm,  $c = 2.0 \times 10^{-5}$  M.

## 8. Photopolymerization Kinetic Investigations

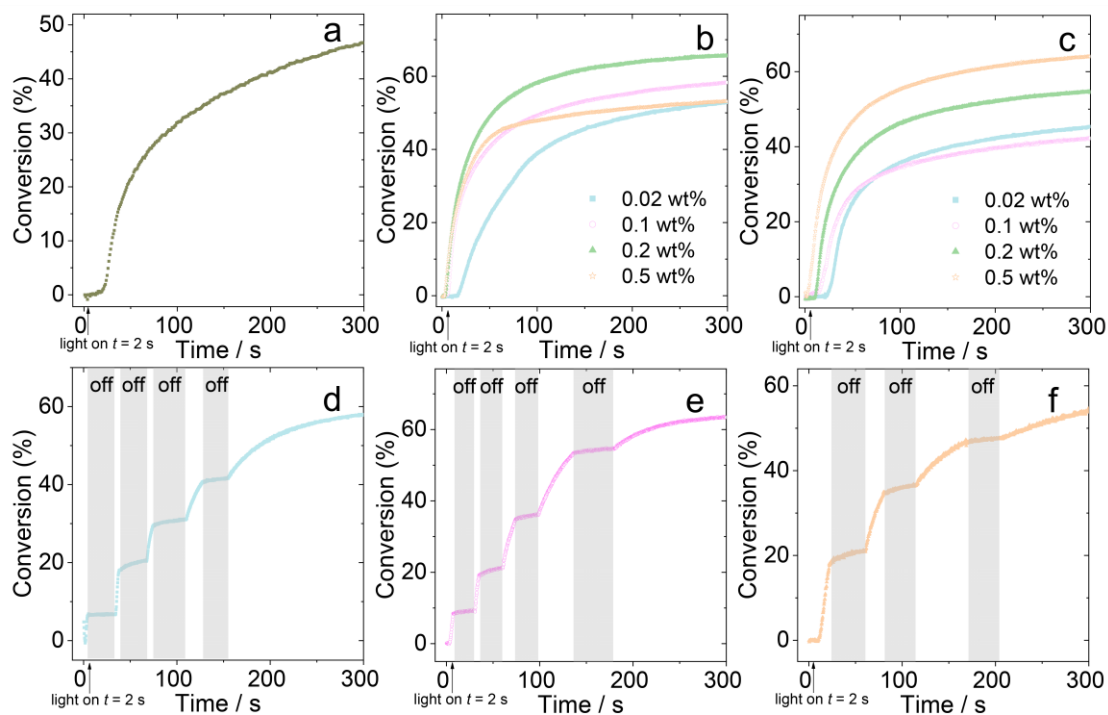


**Figure S29.** Photopolymerization profiles of PETA under the slide at (a) DPI, different concentration of (b) **PSeZ-DTO** and (c) **DPTZ-DTO**. Photopolymerization profiles of PETA upon intermittent switching UV light on / off in the presence of (d) **PTZ-DTO**, (e) **PSeZ-DTO** and (f) **DPTZ-DTO**. Photosensitizer/DPI (0.2 w%/1.0 w%). The light source at 365 nm with 30 mW/cm<sup>2</sup> irradiation intensity. The irradiation starts at  $t = 2$  s. Arrows indicate start of irradiation.

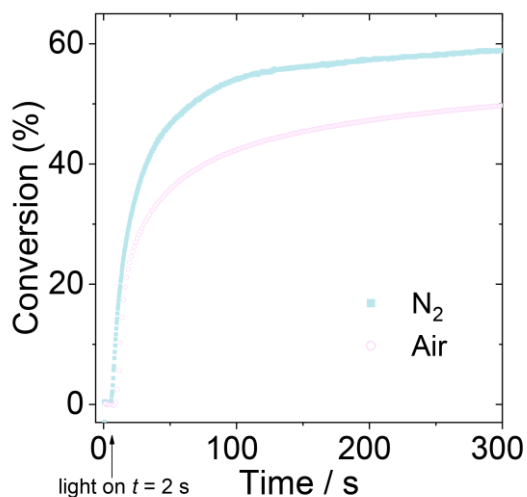


**Figure S30.** Photopolymerization profiles of PETA under the N<sub>2</sub> and Air. **PTZ-DTO/DPI** (0.2 w%/1.0 w%). The light source at 365 nm with 30 mW/cm<sup>2</sup> irradiation intensity. The irradiation starts at  $t = 2$  s. Arrows indicate start of irradiation.

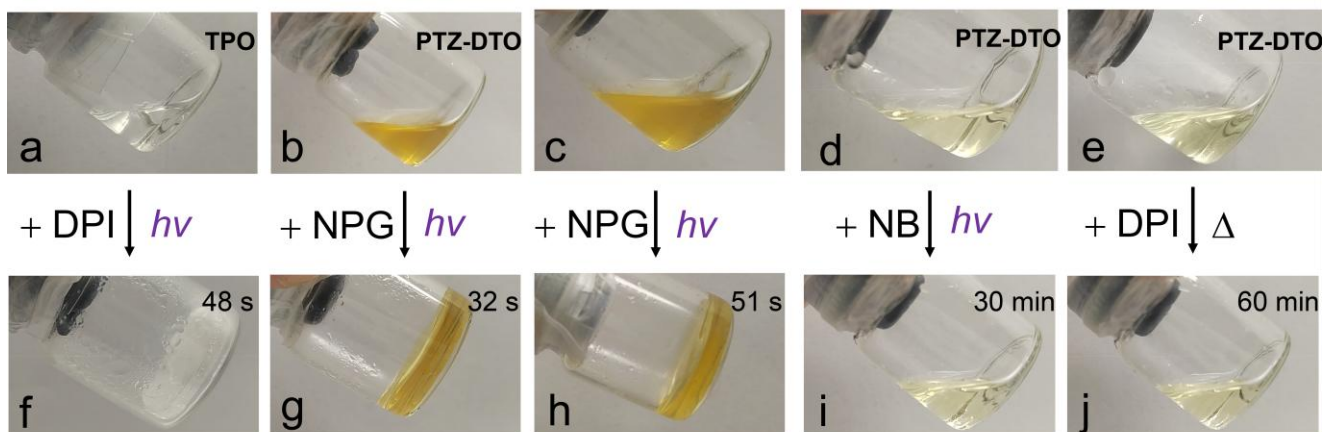


**Figure S31.** The photopolymerization of PETA under N<sub>2</sub> before irradiation in the presence of (a) 2,4,6-trimethylbenzoyldiphenyl phosphine oxide (TPO)/DPI (0.2 wt%/1.0 wt%), (b) **PTZ-DTO**/N-Phenylglycine (NPG) (0.2 wt%/1.0 wt%), (c) only NPG (1.0 wt%), (d) **PTZ-DTO**/tetrabutylammonium tris(3-chloro-4-methylphenyl)hexylborate (NB) (0.2 wt%/1.0 wt%). The polymerization of PETA under N<sub>2</sub> before heating in the presence of (e) **PTZ-DTO**/DPI (0.2 wt%/1.0 wt%). The photopolymerization of PETA under N<sub>2</sub> after irradiation using 30 mW/cm<sup>2</sup> upon 365 nm LED of (f), (g), (h), (i). The polymerization of PETA under N<sub>2</sub> after heating of (j).

## 9. Reference

- 1 L. Deng, L. Tang, J. Qu, *Prog. Org. Coat.* **2022**, *167*, 106859.
- 2 C. Cremer, A. M. Eltester, H. Bourakhouadar, I. L. Atodiresei, F. W. Patureau, *Org. Lett.* **2021**, *23*, 3243–3247.
- 3 Y. Pei, A. A. Sukhanov, X. Chen, A. Iagatti, S. Doria, X. Dong, J. Zhao, Y. Li, W. Chi, V. K. Voronkova, M. Di Donato, B. Dick, *Chem. Eur. J.* **2025**, *31*, e20240354.
- 4 R. S. Nobuyasu, Z. Ren, G. C. Griffiths, A. S. Batsanov, P. Data, S. Yan, A. P. Monkman, M. R. Bryce, F. B. Dias, *Adv. Opt. Mater.* **2016**, *4*, 597–607.
- 5 S. Xu, B. Liu, *J. Am. Chem. Soc.* **2022**, *144*, 17897–17904.
- 6 M. K. Etherington, F. Franchello, J. Gibson, T. Northey, J. Santos, J. S. Ward, H. F. Higginbotham, P. Data, A. Kurowska, P. L. Dos Santos, D. R. Graves, A. S. Batsanov, F. B. Dias, M. R. Bryce, T. J. Penfold, A. P. Monkman, *Nat. Commun.* **2017**, *8*, 14987.
- 7 H. Gilman, J. F. Nobis, *J. Am. Chem. Soc.* **1945**, *67*, 1479–1480.